International Journal of Electrical, Electronic and Communication Sciences
ISSN: 2517-9438
Vol:4, No:6, 2010

Fault Detection of Broken Rotor Bars Using Stator Current Spectrum for the Direct Torque Control Induction Motor

Ridha Kechida, Arezki Menacer, Abdelhamid Benakcha

Abstract**—**The numerous qualities of squirrel cage induction machines enhance their use in industry. However, various faults can occur, such as stator short-circuits and rotor failures.

In this paper, we use a technique based on the spectral analysis of stator current in order to detect the fault in the machine: broken rotor bars. Thus, the number effect of the breaks has been highlighted. The effect is highlighted by considering the machine controlled by the Direct Torque Control (DTC). The key to fault detection is the development of a simplified dynamic model of a squirrel cage induction motor taking account the broken bars fault and the stator current spectrum analysis (FFT).

Keywords**—**Rotor faults, diagnosis, induction motor, DTC, stator current spectrum.

I. Introduction

ROTOR cage faults are the third most important failure cause in induction motors. These failures are motivated by a combination of internal and external stresses, acting together with the natural aging process of the motor [1].

Rotor cage faults can be a serious problem when induction motors have to perform hard duty cycles. If they do not initially cause an induction motor to fail, they can impair motor performance, lead to motor malfunction, and cause serious mechanical damage to stator windings if left undetected. Moreover, an induction motor with broken rotor bars cannot operate in dangerous environments due to sparking at the fault site [1]. For these reasons, a substantial amount of research has been devoted to this topic in the past decades, in order to create new condition monitoring techniques for electrical machine drives, with new methods being developed and implemented in commercial products for this purpose [2]-[3].

The research and development of newer and alternative diagnostic techniques is continuous, however, since condition monitoring and fault diagnosis systems should always suit new specific electric motor drive applications [2], [3].

This work is realized at the LGEB laboratory (Laboratory of Electrical Engineering of Biskra, Algeria) by Dr Arezki Menacer, Dr Abedelhamid Benakcha, at the Department of Electrical Engineering, University Mohamed Khider, BP 145, 07000, Biskra, Algeria

Ridha Kechida (e-mail: ridha.k84@gmail.com).
Arezki .Menacer (e-mail menacer_arezki@hotmail.com).
Abdelhamid .Benakcha (e-mail: benakcha_a@yahoo.fr).

DTC (Direct Torque Control) is characterized, as deduced from the name, by directly controlled torque and flux and indirectly controlled stator current and voltage. It is an alternative dynamic control for vector control. The big interest in DTC is caused by some advantages in comparison with the conventional vector-controlled drives [4]. This control technique provides remarkable dynamic performance for parametric variations produced by many faults in the machine (rotor failures).

II. Model of the Induction Motor [5, 6]

The model of the induction motor takes into account the following assumptions:

- negligible saturation and skin effect,
- uniform air-gap,
- sinusoidal mmf of stator windings in air-gap,
- rotor bars are insulated from the rotor, thus no inter-bar current flows through the laminations,
- relative permeability of machine armatures is assumed infinite.

Although the mmf of the stator windings supposed is to be sinusoidal, other distributions of rolling up could also be considered by simply employing the superposition theorem. It is justified by the fact that the different components of the space harmonics do not interact.

In order to study the phenomena taking place in the rotor, the latter is often modeled by N_R meshes as shown on figure 1.

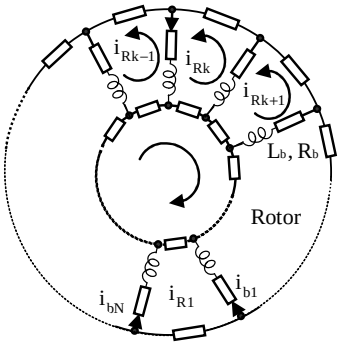

Fig.1. Rotor cage equivalent circuit

A. Stator inductance

The expression of mmf a phase "a" is given by the following:

$$F_m(\theta) = \frac{2N_s i_a}{p\pi}\cos(\theta) \quad (1)$$

The induction created in the air-gap can be written as:

$$B_s(\theta) = \frac{2\mu_0 N_s i_a}{ep\pi}\cos(\theta) \quad (2)$$

The main flux is thus written as:

$$\phi_{sp} = \frac{4\mu_0 N_s^2 RL}{\pi ep^2} i_a \quad (3)$$

The principal inductance of the magnetizing stator phase is:

$$L_{sp} = \frac{\phi_{sp}}{i_a} = \frac{4\mu_0 N_s^2 RL}{\pi ep^2} \quad (4)$$

Therefore the total inductance of a phase is equal to the sum of the magnetizing and leakage inductances, thus:

$$L_s = L_{sp} + L_{sf} \quad (5)$$

The mutual inductance between the stator phases is computed as:

$$M_s = -\frac{L_s}{2} \quad (6)$$

B. Rotor inductance

The form of the magnetic induction produced by a rotor mesh in the air-gap is supposed to be radial and is represented in Fig. 2. The principal inductance of a rotor mesh can be calculated from the magnetic induction distribution shown in figure 2 [5, 6]:

$$L_{rp} = \frac{N_r - 1}{N_r^2}\mu_0 \frac{2\pi}{e} RL \quad (7)$$

The total inductance of the k^{th} rotor mesh is equal to the sum of its principal inductance, inductance of leakage of the two bars and inductance of the leakage of the two portions of rings of the short circuit closing the mesh k as indicated in figure 3.

$$L_{rr} = L_{rp} + 2L_b + 2L_e \quad (8)$$

$$M_{rr} = -\frac{1}{N_r^2}\frac{2\pi\mu_0}{e} RL \quad (9)$$

The k^{th} mutual inductance between the adjacent meshes is given by:

$$M_{rk(k-1)} = M_{rk(k+1)} = M_{rr} - L_b \quad (10)$$

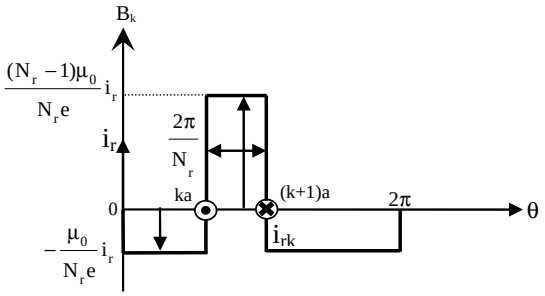

Fig.2. Form of magnetic induction of rotor mesh created by two bars

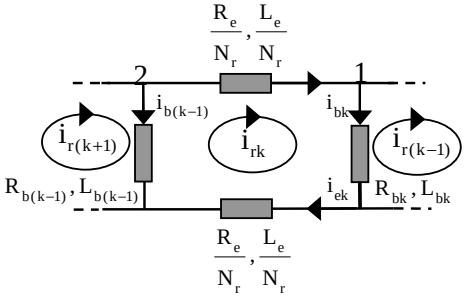

Fig.3. Electric diagram equivalent of a rotor mesh

The expression for the mutual inductance stator-rotor is can be calculated using the flux and is given by:

$$M_{snrk} = -M_{sr}\cos(p\theta_r - n\frac{2\pi}{3} + ka) \quad (11)$$

where:

$$a = p\frac{2\pi}{N_r} \text{ and } M_{sr} = \frac{4\mu_0 N_s Rl}{ep^2\pi}\sin(\frac{a}{2})$$

The representation of state is apparently a system of very high order. The application of transformation the Park's extended of rotor system so as to transform the system in Nr phases in a system (d,q).

We obtain a model of reduced size of the induction machine. The system is put in the following canonical form:

$$[L]\frac{d[I]}{dt} = [V] - [R][I] \quad (12)$$

where:

$$[L] = \begin{bmatrix} L_{sc} & 0 & -\frac{N_r}{2}M_{sr} & 0 & 0 \\ 0 & L_{sc} & 0 & -\frac{N_r}{2}M_{sr} & 0 \\ -\frac{3}{2}M_{sr} & 0 & L_{rc} & 0 & 0 \\ 0 & -\frac{3}{2}M_{sr} & 0 & L_{rc} & 0 \\ 0 & 0 & 0 & 0 & L_e \end{bmatrix},$$

$$[R] = \begin{bmatrix} R_s & -L_{sc}\omega_r & 0 & \frac{N_r}{2}M_{sr}\omega_r & 0 \\ L_{sc}\omega_r & R_s & -\frac{N_r}{2}M_{sr}\omega_r & 0 & 0 \\ 0 & 0 & R_r & 0 & 0 \\ 0 & 0 & 0 & R_r & 0 \\ 0 & 0 & 0 & 0 & R_e \end{bmatrix},$$

$$L_{rc} = L_{rp} - M_{rr} + \frac{2.L_e}{N_r} + 2.L_e\left(1-\cos(a)\right)$$

and

$$R_r = 2\frac{R_e}{N_r} + 2.R_b\left(1-\cos(a)\right)$$

In order to simulate the defect of rotor broken bars, a fault resistance R_{RF} is added to the corresponding element of the rotor resistance matrix R_r:

$$[R_F] = \begin{bmatrix} 0 & \cdots & & 0 & 0 & 0 & \cdots \\ \vdots & \cdots & & \vdots & \vdots & & \cdots \\ 0 & \cdots & 0 & 0 & 0 & 0 & \cdots \\ 0 & \cdots & 0 & R_{bk} & -R_{bk} & 0 & \cdots \\ 0 & \cdots & 0 & -R_{bk} & R_{bk} & 0 & \cdots \\ 0 & \cdots & 0 & 0 & 0 & 0 & \cdots \\ \vdots & \vdots & \vdots & \vdots & \vdots & 0 & \cdots \end{bmatrix}$$

Consequently, the squirrel cage resistance matrix, taking into account the defect, is defined by:

$$[R_{RF}]_{N_R \times N_R} = [R_R]_{N_R \times N_R} + [R_F]_{N_R \times N_R} \quad (13)$$

The new matrix of rotor resistances, after transformations, becomes:

$$[R_{RF}] = \begin{bmatrix} R_{rdd} & R_{rdq} \\ R_{rqd} & R_{rqq} \end{bmatrix} \quad (14)$$

where the four terms of this matrix are:

$$R_{rdd} = 2R_b\left(1-\cos(a)\right) + 2\frac{R_e}{N_r} + \frac{2}{N_r}\left(1-\cos(a)\right)\sum_k R_{bfk}\left(1-\cos(2k-1)a\right)$$

$$R_{rdq} = -\frac{2}{N_r}\left(1-\cos(a)\right)\sum_k R_{bfk}\sin(2k-1)a$$

$$R_{rqd} = -\frac{2}{N_r}\left(1-\cos(a)\right)\sum_k R_{bfk}\sin(2k-1)a$$

$$R_{rqq} = 2.R_b\left(1-\cos(a)\right) + 2\frac{R_e}{N_r} - \frac{2}{N_r}\left(1-\cos(a)\right)\sum_k R_{bfk}\left(1-\cos(2k-1)a\right)$$

"k" characterizes the position of broken bar

The equations governing the operation of asynchronous motor with or without rotor defects become $[R']$:

$$[R'] = \begin{bmatrix} R_s & -L_{sc}\omega_r & 0 & \frac{N_r}{2}M_{sr}\omega_r & 0 \\ L_{sc}\omega_r & R_s & -\frac{N_r}{2}M_{sr}\omega_r & 0 & 0 \\ 0 & 0 & \lceil R_{rdd} & R_{rdq}\rceil & 0 \\ 0 & 0 & \lfloor R_{rqd} & R_{rqq}\rfloor & 0 \\ 0 & 0 & 0 & 0 & R_e \end{bmatrix}$$

The mechanical equations must also consider:

$$\frac{d}{dt}\omega = \frac{1}{J}(C_e - C_r) \quad (15)$$

with: $\omega = \frac{d\theta}{dt}$

The electromagnetic torque with the expression:

$$Ce = \frac{3}{2}p.N_r.M_{sr}\left(I_{ds}.I_{qr} - I_{qs}.I_{dr}\right) \quad (16)$$

III. Direct Torque Control for the Machine with Rotor Faults

DTC is a control philosophy exploiting the torque and flux producing capabilities of ac machines when fed by a voltage source inverter that does not require current regulator loops, still attaining similar performances to that obtained by a vector control drive [7].

The typical structure of a DTC induction motor is presented in figure .4.

A. Behavior of stator flux

In the reference (α,β), the stator flux can be obtained by the following equation:

$$\bar{V}_s = R_s.\bar{i}_s + \frac{d}{dt}\bar{\phi}_s \quad (17)$$

By neglecting the voltage drop due to the resistance of the stator to simplify the study (for high speeds), we find:

$$\bar{\phi}_s \approx \bar{\phi}_{s0} + \int_0^t \bar{V}_s dt \quad (18)$$

Table I: Selection table for direct torque control

Cflx	1	1	1	0	0	0
Cclp	1	0	-1	1	0	-1
S_1	V_2	V_7	V_6	V_3	V_0	V_5
S_2	V_3	V_0	V_1	V_4	V_7	V_6
S_3	V_4	V_7	V_2	V_5	V_0	V_1
S4	V_5	V_0	V_3	V_6	V_7	V_2
S_5	V_6	V_7	V_4	V_7	V_0	V_3
S_6	V_1	V_0	V_5	V_2	V_7	V_4

B. Behavior of the torque

The electromagnetic torque is proportional to the vector product between the stator and rotor flux according to the following expression [8]:

$$C_e = k\left(\bar{\phi}_s \times \bar{\phi}_r\right) = k\left|\bar{\phi}_s\right|\left|\bar{\phi}_r\right|\sin\theta_{sr} \quad (19)$$

C. Development of the commutation strategy

Table 1, shows the commutation strategy suggested [9], to control the stator flux and the electromagnetic torque of the stator of induction machines.

Figure 4 gives the partition of the complex plan in six angular sectors $S_{I=1...6}$.

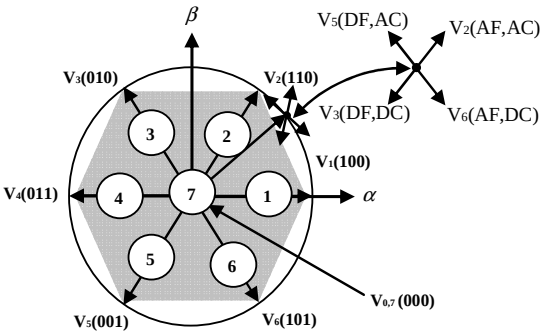

Fig 4: Partition of the complex plan in six angular

IT: Increase the Torque, DT: Decrease the Torque.
IF: Increase the Flux, DF: Increase the Flux.

IV. Simulation Results

The simulations of the DTC induction motor drive were carried out using the Matlab / Simulink simulation package. The motor used in the simulation study is a 1.1 kW, 220 V, 50 Hz, 2-pole induction motor, with a rotor with 16 bars.

A. Inversion of the speed and variation of the torque

The test robustness of the system, we applied a changing of the speed reference from 100 rad/sec to -100 rad/sec at t=1s with load of torque 3.5 N.m at t=0.5s and t=1.5s (Fig 5). During the Inversion of the speed, the torque present exceeded before stabilizing. The stator currents present undulations at the moment of the inversion comparable with the peak during starting.

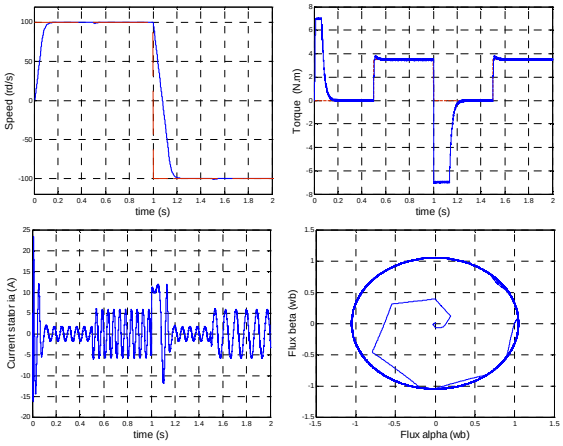

Fig.5. Inversion of speed and variation of the torque load test

B. the reference trapezoidal wave speed

Simulations are performed to validate the proposed DTC for four-quadrant speed control of induction machine. The square wave of speed references is tested. Figure 6 show the response trapezoidal wave speed references respectively.

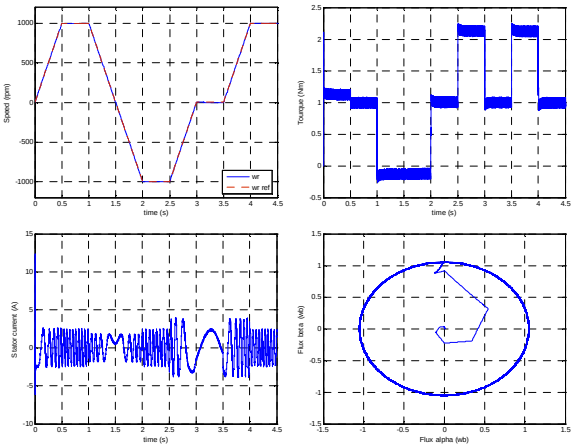

Fig.6. Trapezoidal wave speed test

C. *Effect of the number of rotor broken bars*

The spectral analysis of stator phase currents highlights the effect of the defect the appearance of through harmonics around the fundamental [5, 6].

Their amplitudes increase according to the number of defective bars at characteristic frequencies (Eq. 20).

$$f_{defect} = (1 \pm 2.n.g) f_s , \qquad n = 1, 2, .. \tag{20}$$

Several quantities were calculated and analyzed in order to access the information they contained about the presence of the simulated fault (one and two broken rotor bars). The motor induction was initially operated with a load torque of 3 Nm and the reference speed was set to 2800 rpm.

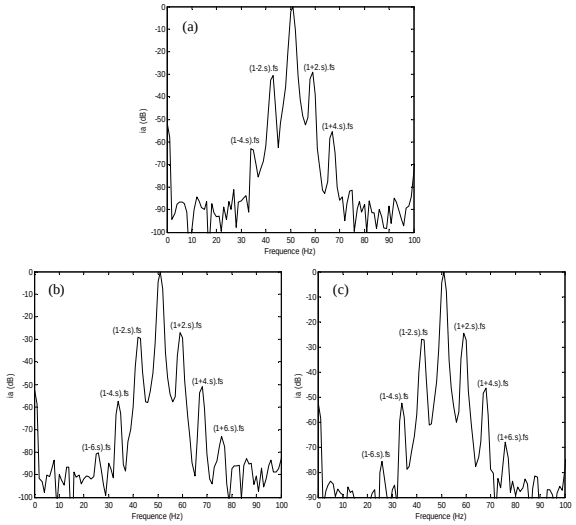

Fig 7: Stator current spectrum for:
(a) One broken bar (b) Spaced two broken bars (c) Adjacent two broken bras

On the figure (7), we notice the appearance of harmonics on the spectrum. These harmonic have amplitude which increases according to the raise of the defective bars number. Table II highlights the influence of the number of broken bars on the stator current spectrum.

D. *Effect of the load*

The effect of the load on the stator current spectrum is highlighted by considering a break of two adjacent bars with different slips (s=0.9%, s=3.48%, s=6.30% and s=7.77%) and the reference speed was set to 2500 rpm (see figure (8)).

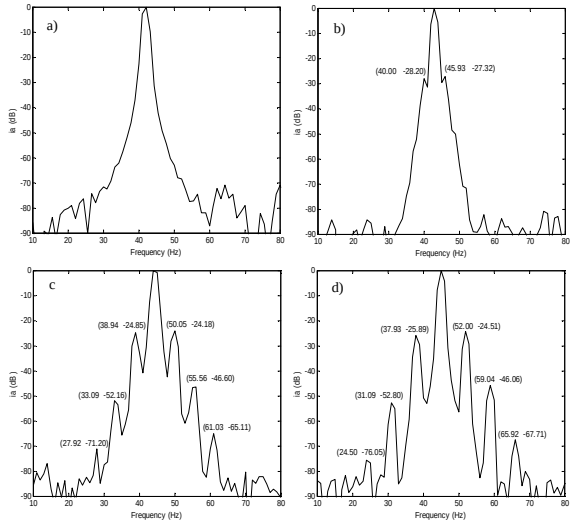

Fig.8. Stator current spectrum with different slips for adjacent two broken rotor bars: a) s=0.9% b) s=3.48% c) s=6.30% d) s=7.77%

We note that the lines due to defect invisible for weak slips (figure 8.a) and less visible with average slip (figure 8.b). So it is difficult to detect the defect of broken bars with weak load. On the other hand, for nominal loads (figure 8.c, d), the lines are visible. We have shown by spectral analysis and monitoring the evolution of characteristic frequencies of a defect present in the stator current could deduce the state of the machine. Indeed, through its control of the speed control of induction machine, we know the speed of mechanical rotation, slip estimate and can therefore easily locate the characteristic frequencies of the lines due to default.

V. Conclusion

This paper presents within the framework of the diagnosis asynchronous motor broken bars simulation based on the development of a reduced model.

The stator current spectrum analysis shows the presence of a defect due to the break or the rupture of bars thanks to appearance of the different harmonics the given by equation (20). Also, by controlling the speed of induction machine, we know that speed mechanical, slip estimate and can not easily locate the characteristic frequencies of the lines due to defect. Further research has to be done in this field in order to make the diagnosis of rotor faults more reliable in this type of drive.

TABLE II
SIMULATION FREQUENCIES AND MAGNITUDES OF THE STATOR CURRENT SPECTRUM:
a) One broken bars b) Spaced two broken bars c) Adjacent two broken bars

		f cal=(1-6s)f_s	f cal=(1-4s)f_s	f cal=(1-2s)f_s	f cal=(1+2s)f_s	f cal=(1+4s)f_s	f cal=(1+6s)f_s
s=7.84 %	calculated f(Hz)	27.009	35.006	43.003	58.548	66.993	74.990
	deduced f (Hz)	27.000	33.927	42.999	58.991	66.994	74.992
	Magnitude (dB)	-81.094	-62.947	-30.622	-28.986	-55.554	-81.429
s=7.95 %	calculated f(Hz)	26.673	34.782	42.891	59.109	67.218	75.327
	deduced f (Hz)	25.477	33.970	42.495	58.990	68.030	75.996
	Magnitude (dB)	-80.555	-57.599	-29.369	-27.125	-50.962	-72.944
s=8 %	calculated f(Hz)	26.489	34.659	42.829	59.170	67.340	75.510
	deduced f (Hz)	26.001	33.968	42.478	58.962	67.940	76.003
	Magnitude (dB)	-75.586	-52.619	-27.093	-24.632	-46.598	-67.946

APPENDIX

For the simulated induction motor

Pn Output power	1.1 kW
Vs Stator voltage	220 V
fs Stator frequency	50 Hz
p Pole number	1
Rs Stator resistance	7.58 Ω
Rr Rotor resistance	6.3 Ω
R_b Rotor bar resistance	0.15 mΩ
Re Resistance of end ring segment	0.15 mΩ
L_{b0} Rotor bar inductance	0.1 µH
Le inductance of end ring	0.1 µH
L_{sf} Leakage inductance of stator	26.5 mH
M_{sr} Mutual inductance	46.42 mH
N_s Number of turns per stator phase	160
N_r Number of rotor bars	16
L Length of the rotor	65 mm
e Air-gap mean diameter	2.5 mm
J Inertia moment	0.0054 kg m^2

REFERENCES

[1] Drif, M.; Cardoso, A. J. M.; "The Instantaneous Reactive Power Approach for Rotor Cage Faults Diagnosis in Induction Motor Drives", Proc *IEEE Power Electronics Specialists Conf. - PESC*, Rhodes, Greece, Vol. 1, pp. 1548 - 1552, June, 2008.

[2] M. Eltabach, A. Chahata and I. Zein, "A comparison of external and internal methods of signal spectral analysis for broken rotor bars detection in induction motors," *IEEE Trans. on Ind. Elec.*, vol. 51, n° 1, pp. 107-121, Feb. 2004.

[3] M. E. H. Benbouzid, "Bibliography on induction motor faults detection and diagnosis," *IEEE Trans. on Energy Conver.*, vol. 14 n° 4, pp. 1065-1074, Dec.1999.

[4] W.S.H. Wong and D. Holliday. "Minimisation of flux droop in direct torque controlled induction motor drives", *IEEE*, 7 Nov 2004, pp. 694-703, proceedings online no. 20040681.

[5] Menacer, A. Benakcha, M.S. Nait Said, S. Drid, "Stator Current Analysis of Incipient Fault into Induction Machine Rotor Bras", *Journal of Electrical Engineering, Roumanie*, Vol 4, N°2-2004, pp 5-12.

[6] Menacer, S. Moreau, A. Benakcha, M.S. Nait Said " Effect of the position and the number of broken bras on Asynchronous Motor Stator Current Spectrum", *EPE-Power Electronics and Motion Control*, Portoroz, Slovenia, 2006.

[7] S. Benaggoune, S. Belkacem, R. Abdessemed, "Sensorless Direct Torque Control of PMSM Drive with EKF Estimation of Speed, Rotor Position and Load Torque Observer", *Asian Journal of Information Technology* 6 (2): 236-242, 2007.

[8] Canudas, " Modélisation Contrôle Vectoriel et DTC ", *Edition HARMES Science Europe, Ltd*.

[9] Takahashi, T. Noguchi, "A New Quick Response and High Efficiency Control Strategy of an Induction Machine", IEEE. Trans. Indus. Applied, 22: 820-827.

Ridha Kechida was born in El-oued, Algeria, in 1984. He receives the B.Sc. degree in electrical engineering from the University of Biskra, Algeria, in 2007, and working to get an the M.Sc. electrical networks from the Science and Technology Institute of El-oued Centre Universitaire, Algeria. His research interests include control of electrical drives, in particular, the direct torque control in asynchronous motors and diagnosis, (ridha.k84@gmail.com).

Menacer Arezki was born in Batna, Algeria, in 1968. He receives the B.Sc. degree in electrical engineering from the University of Batna, Algeria, in 1992, and the M.Sc. degree in electrical control from the Electrical Engineering Institute of Biskra University, Algeria, in 1996. He receives the Ph.D. degree in electrical control from the University of Batna and LAII Laboratory of Automatic and Industrial data processing, University of Poitiers, France, in 2007 and the "habilitation degree" in 2009 from University of Biskra Algeria. Currently, he is a Teaching Assistant with the Electrical Engineering Institute at the University of Biskra and member of LGEB Laboratory of Electrical Engineering of Biskra, Algeria. His major fields of interest in research are diagnosis, identification and control of electrical machines. (menacer_arezki@hotmail.com).

Benakcha A/Hamid was born in 1961 in Arris, Algeria. He had achieved a M.sc. in 1980 and a B.Sc. in 1983 from the University of Batna, Algeria, and a Master of Science in 1985 and a Ph.D. in electronics from the University of Clermont-Ferrand, France. Since 1991, he teaches at the University of Biskra, Algeria. He is member of the Research Laboratory of electrotechnic of Biskra and the head of the research group: Simulation of sliding mode control of an asynchronous machine. His other research interests are: Electric machines (design, modelling, identification, control), power electronics, electromagnetism (antennas, free propagation), electronics (television). (benakch_a@yahoo.fr)